Monitoring Gold Nanorod Synthesis on Surfaces

Hongwei Liao[†] and Jason H. Hafner*[,†,‡]

Departments of Chemistry and Physics & Astronomy, Rice University, 6100 Main Street, Houston, Texas 77005

Received: August 15, 2004; In Final Form: September 14, 2004

We describe a simplified method for the synthesis of gold nanorods on surfaces. Gold colloid seeds were deposited by electrostatic attraction onto silicon wafers and grown in a $HAuCl_4$ solution by surfactant-assisted, seed-mediated synthesis. Microscopic analysis of the nanoparticle ensemble allowed direct observation of several aspects of the anisotropic growth of gold nanorods. Individual seed particles were observed to produce individual nanorods with yields similar to those of previous reports with the seed particles in solution. A minimum seed diameter of 17 nm was required for nanorod nucleation, and this minimum was the same for surfactants with both 12- and 16-carbon chains. However, the chain length affected the isometric seed growth rate, which was faster for the shorter chain surfactant. Altering the surfactant headgroup disrupted the growth anisotropy and produced no nanorods.

Introduction

The optical properties of metallic nanoparticles have generated recent interest for their applications in a variety of areas including enhanced spectroscopies,[1] molecular electronics,[2] gene delivery,[3] chemical sensors,[4,5] and photothermal cancer therapy.[6] The plasmon resonance energy can be tuned by adjusting the nanoparticle size and shape. For example, gold nanorods have optical plasmon resonances that can be tuned rationally through the visible and near-IR on the basis of their aspect ratio.[7] Several synthetic strategies have been recently developed for simple, wet chemical synthesis of gold nanorods with shape control mediated by templates including porous inorganic substrates,[8] polycarbonate membranes,[9] and surfactants.[10] A particularly versatile method is seed-mediated growth in the presence of a surfactant.[11−13] In this method a seed solution of 3−4 nm diameter gold nanoparticles is prepared by the reduction of $HAuCl_4$ in the presence of $NaBH_4$ with a citrate capping agent. A growth solution is also prepared with $HAuCl_4$, ascorbic acid (a weak reduction agent), and the surfactant cetyltrimethylammonium bromide (C_{16}TAB). While the growth solution will not form particles on its own, the addition of the seed solution results in growth of the seed particles by the reduction of gold on their surface.[14] The growth of the spherical seed particles into nanorods is not understood in detail, but its origin apparently lies in the relative binding strength of C_{16}TAB bilayers to different nanoparticle crystal facets, thus creating anisotropic growth conditions.[15−17] Several studies have introduced variations in the synthesis aimed at understanding the mechanism and improving the yield and aspect ratio. These include altering the capping agent,[18] adding a small percentage of silver ions,[13,19] varying the surfactant chain length and headgroup,[20] using binary surfactant mixtures,[18] and adjusting the pH of the growth solution.[21] While these studies continue to shed light on the growth process and improve the product, several questions remain regarding the growth mechanism. A complete understanding of the synthesis reaction is vital since it could lead to higher yields and better control of the size and shape, which greatly influence the optical properties.

Gold nanorods have been grown from seed particles bound to aminopropyltrimethoxysilane (APTMS) monolayers on mica substrates rather than in bulk solution.[22] This demonstration represented a first step toward the synthesis of gold nanorod arrays directly into device architectures for nanoelectronics. In a recent report nanorods were grown on seeds bound to mercaptopropyltrimethoxysilane (MPTMS) monolayers on glass, achieving higher aspect ratios through larger $HAuCl_4$ concentrations in the growth solution.[23] The motivation of our work is to exploit the surface growth method to investigate nanorod synthesis mechanisms. We introduce a significant simplification for the preparation of the seeded substrate—the use of commercially available gold colloid particles deposited by simple electrostatic attraction—thus removing sensitive steps of borohydride reduction and organic monolayer formation. This simplified procedure, coupled with microscopic analysis of the nanoparticle products, is ideal for studying the growth mechanisms of nanorod synthesis.

Methods

n-doped silicon wafers (⟨100⟩, 0.01 Ω cm) with native oxide were cleaned with methanol, dipped in 0.01% w/v poly-L-lysine for 10 min, and rinsed with DI water. The silicon chips were covered with 20 μL of commercially available gold colloid solution (Ted Pella, Redding, CA) for 10 min and then rinsed with DI water. The nominal colloid diameters (nm) at various concentrations (particles/mL) were 2 at 1.5×10^{14}, 5 at 5.0×10^{13}, 10 at 5.7×10^{12}, 15 at 1.4×10^{12}, and 20 at 7.0×10^{11}. The seeded substrates were then placed in a glass Petri dish with 10 mL of 0.06 M C_{16}TAB solution for 5 min. Next, 0.5 mL of 0.25 mM $HAuCl_4$ was added, immediately followed by 50 μL of 10 mM ascorbic acid. The reaction was allowed to proceed for the growth time, up to 60 min, and the substrates were removed and rinsed with DI water. Identical reactions were also carried out with dodecyltrimethylammonium bromide (C_{12}TAB) and cetylpyridinium chloride (C_{16}PC) as the surfactants. The resulting metal nanoparticles were analyzed by scanning electron microscopy (SEM; JEOL 6500F) and atomic

* To whom correspondence should be addressed. E-mail: hafner@rice.edu.
† Department of Chemistry.
‡ Department of Physics & Astronomy.

10.1021/jp046328m CCC: $27.50
Published on Web 11/12/2004

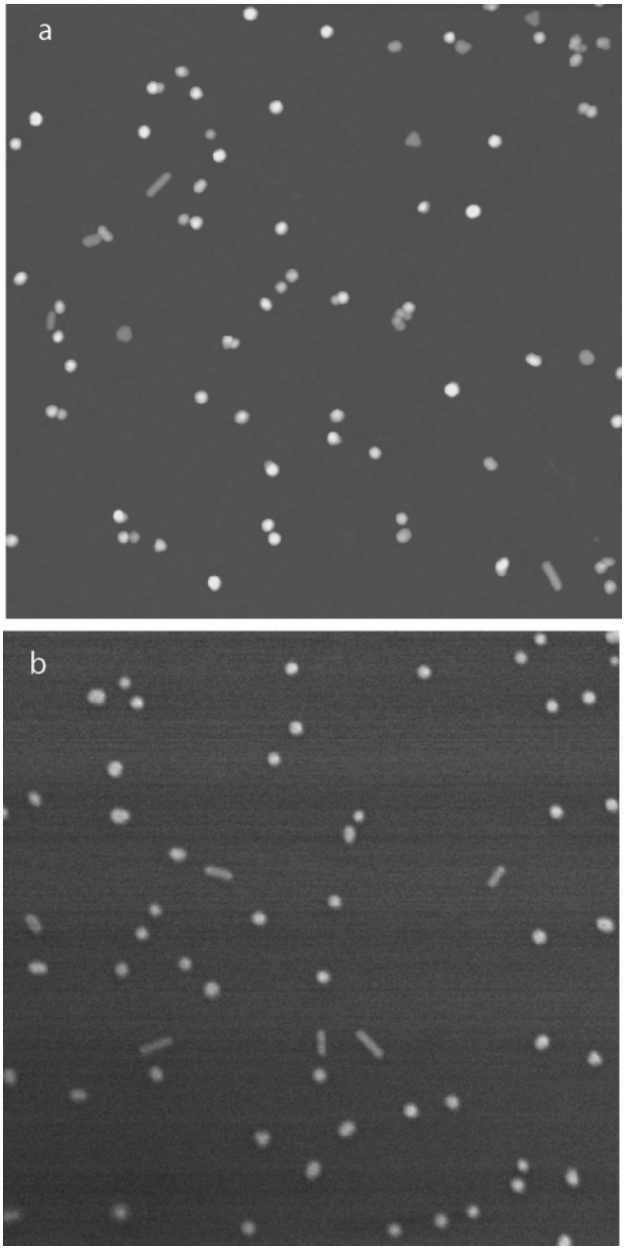

Figure 1. AFM (a) and SEM (b) images of gold nanorods grown from 10 nm colloid seeds supported on a silicon wafer in the presence of C_{16}TAB, $HAuCl_4$, and ascorbic acid for 60 min. The scan size is 2 × 2 μm, and height in the AFM image is represented by a 50 nm linear gray scale.

force microscopy (AFM) in tapping mode at random positions on the wafer with 2 μm scans (Veeco Multimode Nanoscope IV). Nanosphere particle counts and diameters were measured with the Nanoscope particle analysis software feature (version 5.12.r3) with a 6 nm threshold height. Error bars on particle diameters represent 1 standard deviation based on a Gaussian fit to the height distributions. The number of nanorods in each image was counted manually and divided by the total particle count to give a percent yield. Since the total particle count, N, was large (greater than 100) and the nanorod count, n, was small (less than 10), the standard deviation of the percent yield was approximated as $100(\sqrt{n})/N$.

Results

Figure 1 shows AFM and SEM images of gold nanorods grown on a silicon wafer for 60 min with 10 nm colloid seeds as described above. Three classes of nanoparticles are visible: nanospheres, nanorods, and triangular shapes (sometimes referred to as nanoprisms[24]). In the AFM images, the aspect ratio of the nanorods is higher than what is apparent due to the well-known tip-induced broadening effect in AFM.[25] Making the approximation that the rods have a circular cross section, although they are most likely pentagonal,[16,17] the tip broadening can be determined by subtracting the measured height (the true diameter) from the width (diameter plus broadening). This value for the tip broadening can then be subtracted from length measurements to determine the true length. The average length and diameter for the sample of Figure 1 are 180 and 19 nm, respectively. Note that these conditions were chosen for simplicity and reproducibility. Other factors known to increase the nanorod aspect ratio and yield have not been tested. To confirm that the nanorods grow from the original deposited seed particles, the same area of a seeded wafer was imaged before and after nanorod synthesis (Figure 2). Of the 10 initial seed particles, 2 formed nanorods while the rest grew into larger nanospheres.

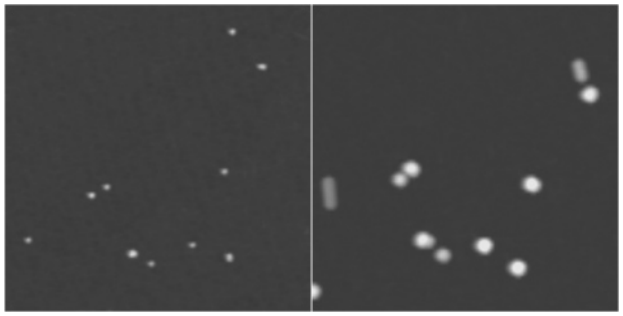

Figure 2. The same area of a wafer with 10 nm gold colloid seeds before (left) and after (right) nanorod growth. The scan size is 1.2 × 1.2 μm, and the linear gray scales represent 20 nm height (before) and 50 nm height (after).

To examine the effect of seed particle diameter on nanorod growth, wafers with 5, 10, 15, and 20 nm diameter Au colloids were prepared and then simultaneously grown in the same solution for 60 min. Figure 3 displays histograms of the measured height and length of the nanorods for each seed size. The products for the 5, 10, and 15 nm seeds had lengths and diameters similar to those of Figure 1, with an aspect ratio of about 10. The 20 nm seeds produced nanorods, but with larger and more varied diameters. The effect of seed diameter on nanorod growth was more directly observed by the following experiment: six wafers seeded with 10 nm gold colloids were placed in growth solution, and one was removed every 10 min, rinsed with DI water, and dried. The wafers were analyzed by AFM to determine the average diameter of the seed particles and the nanorod yield, which are plotted in Figure 4. One clearly observes a continuous growth of the seeds with time in Figure 4a, saturating at 23 nm, which is similar to the nanosphere size observed in Figure 1. In Figure 4b, the plot of nanorod yield reveals that most nanorod nucleation occurs between 20 and 30 min. If one considers the seed particle diameter at this time, it shows that nanorod nucleation preferentially occurs at a seed diameter around 17, in agreement with the results of Figure 3.

Repeating these time-lapsed measurements yields generally similar results, yet there is some variation due to the density of seed particles on the surface. When there is a higher density of seed particles, the nanosphere growth occurs more slowly, and the nanorod nucleation therefore occurs later. To account for these growth rate differences and compare results obtained with different experimental conditions, the seed diameter can be

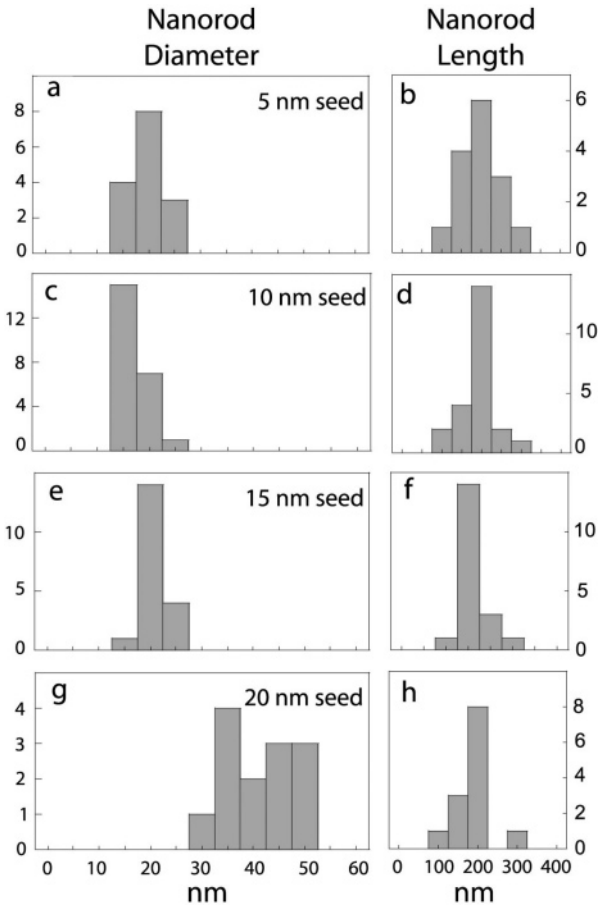

Figure 3. Histograms of nanorod diameters and lengths by synthesis with varying seed sizes. The vertical axis represents the absolute number of nanorods counted.

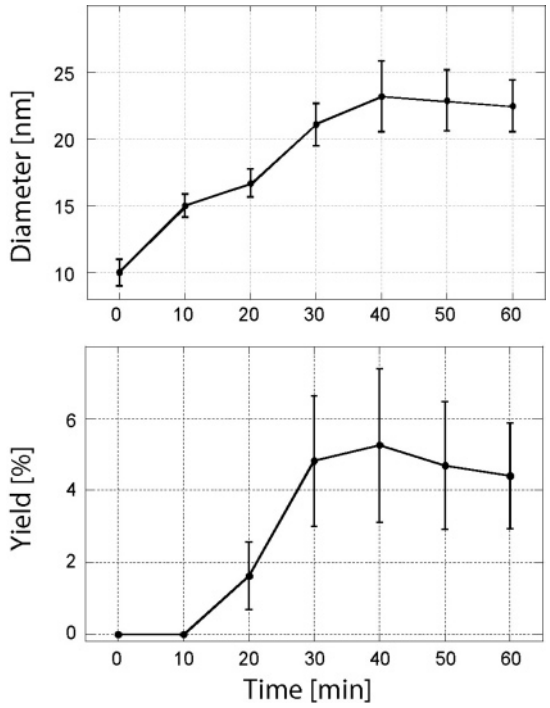

Figure 4. Nanosphere diameter and nanorod yield monitored throughout a 1 h growth experiment in C_{16}TAB.

thought of as a normalized reaction clock. When one plots nanorod yield versus seed particle diameter for multiple runs (Figure 5), one sees that the nucleation always occurs at a seed

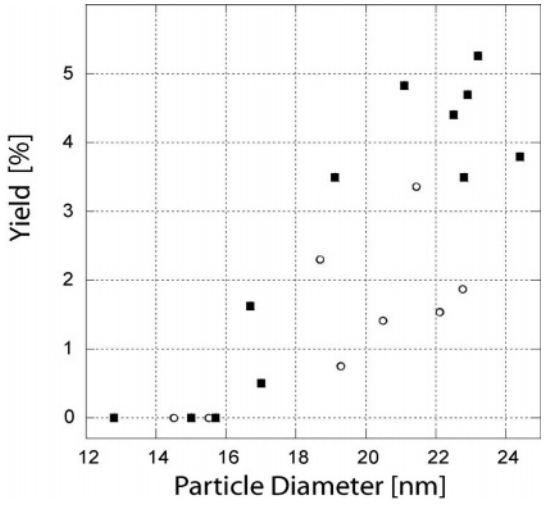

Figure 5. Nanorod nucleation as a function of nanosphere diameter from multiple experiments with C_{16}TAB (squares) and C_{12}TAB (circles). Error bars are similar to those of Figure 4, but are not shown for clarity.

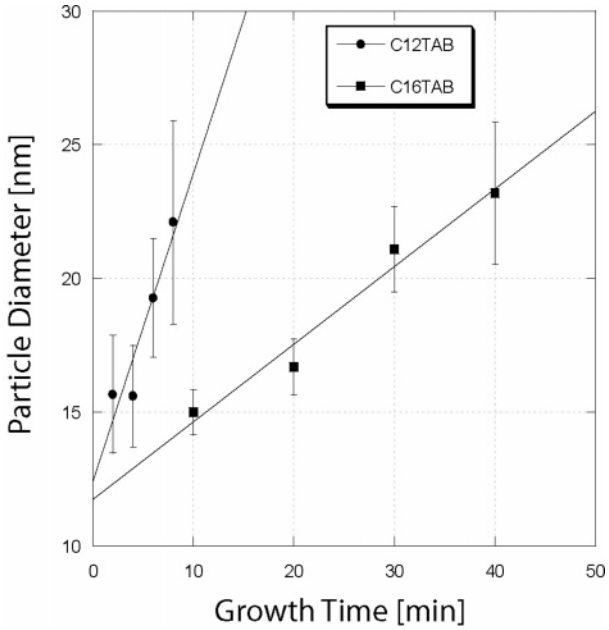

Figure 6. Isometric nanosphere growth rate for C_{16}TAB (squares) and C_{12}TAB (circles).

diameter of 16−18 nm, even though nucleation may have occurred at varying times. These time-lapsed nanorod yield measurements were also carried out with C_{12}TAB. The results, also plotted in Figure 5, demonstrate that the critical size for nanorod nucleation is similar to that for C_{16}TAB. However, if one compares the growth rate of the spherical particles for C_{12}TAB and C_{16}TAB runs with similar seed density, one finds that the shorter chain C_{12}TAB permits faster growth (Figure 6).

Discussion

In seed-mediated gold nanorod synthesis, 3−4 nm gold seed particles grow in solution by the reduction of Au^+ on their surface in the presence of a surfactant. Nanorod formation is thought to occur due to growth anisotropy created on some fraction of the seeds by different surfactant interactions with different crystalline facets and defects on the seed particles.[16] Particles that do not form nanorods grow isometrically into nanospheres. The seed-mediated model is largely based on

spectroscopic evidence showing that C_{16}TAB bilayers are bound to the seed particles during synthesis,[15] and microscopic evidence showing that nanorods grow in the ⟨110⟩ direction with pentatwinned defects.[16,17] The data supporting the seed-mediated model were gathered on nanorod solutions as synthesized or after their transfer to TEM grids. Gold nanorod synthesis by similar chemistry, but on flat substrates,[22,23] provides several advantages for studying the seed-mediated growth mechanism. First, the effective concentration of seed particles is greatly reduced, so they do not deplete the growth solution. This allows the reaction to proceed under more constant and controlled conditions than with seed particles in solution. Second, the reaction can be quenched rapidly by rinsing the substrate with DI water to remove growth solution and surfactant. Third, surface growth yields and shape distributions are determined quantitatively since microscopic analysis takes place with little perturbation of the particle ensemble. This is significant since transfer of a sample from a bulk solution to a TEM grid can be a source of selectivity, possibly creating systematic errors in yield and shape measurements. However, note that the comparison of results from seeds in solution to those from surface-bound seeds assumes that nanorod formation follows the same growth mechanism for each case. Concentrated C_{16}TAB solutions are known to form bilayers on silica surfaces at high concentration,[26] so it is possible that the substrate will have some effect on seed−C_{16}TAB interactions. Figures 1, 3, and 4 show that the substrate synthesis product is very similar to that from solution-based growth in terms of nanorod size and nanorod yield. We therefore assume that the surface and bulk syntheses follow a similar anisotropic growth mechanism, including enhanced growth along the ⟨110⟩ direction.

The simplest view of nanorod growth on surfaces is that the intentionally deposited surface-bound seed particles form surface-bound nanorods while immersed in the growth solution. However, several other mechanisms that may occur on the surface should be considered.[23] For example, the growth solution may contain some small particles (as an impurity) that deposit on the surface and grow to form nanorods. Alternatively, even if the growth solution is free of particles, the seeds or the mica surface may catalyze the formation of gold particles in the growth solution, and these new particles could deposit and grow nanorods on the surface. While some of these possibilities can be ruled out indirectly, Figure 2 explicitly demonstrates that, under the conditions reported here, the original seed particles do indeed form nanorods by addition of gold from the growth solution. Also note that no new particles are observed to deposit from the growth solution. Since nanorod nucleation is thought to require twinned seed particles, seed aggregation as a source of twinning may be an important step of nanorod synthesis.[16] Figure 2 demonstrates that seed aggregation was not necessary for nanorod growth. However, the 10 nm seed is large enough that it is most likely already twinned.[27] A more revealing experiment would be to show that the 5 nm seeds, too small to support twin defects, grow without aggregation. Unfortunately, we found that the electrostatic binding is insufficient for the 5 nm seed particles. The density of nanorods and nanospheres after growth was typically lower than the original seed density, suggesting desorption of the smaller particles. Therefore, direct before/after images could not be compared.

Figures 3 and 4 suggest that there is a critical seed diameter range for facile nanorod nucleation and growth. Since the 5, 10, and 15 nm seeds form similar nanorod products, they must initially grow isometrically and initiate nanorod growth at a similar size. The critical seed size must therefore be greater than 15 nm. Since the monodisperse nanorod product has a diameter of 20 nm, an upper limit to the critical size of 20 nm is appropriate. Note that, above 20 nm, nanorod nucleation clearly still occurs since the 20 nm seeds did form nanorods. However, the more varied product and large sizes suggest that this growth follows a different mechanism, or is controlled by different energetics. The critical size is more clearly demonstrated in the time series measurements of Figure 4. Most of the 10 nm seed particles grew isometrically into larger spheres of 22 nm diameter. Nanorod formation began after 10−30 min, when the average particle size was between 15 and 22 nm. Figure 5, which contains data from multiple reactions, more precisely demonstrates the critical minimum size to be 17 nm, while nucleation ceases once the seeds reach a 20 nm diameter.

The effect of the surfactant has been studied by varying its tail length and headgroup. Growth was carried out with C_{16}PC as the surfactant, which has a 16-carbon chain tail, but a larger headgroup than C_{16}TAB and a counterion different from that of C_{16}TAB. No nanorods were observed from growth in C_{16}PC, as reported previously.[20] This suggests that the alkyltrimethylammonium headgroup contributes to the anisotropic surfactant binding, which leads to nanorod nucleation. In another set of experiments, the headgroup was kept constant and the carbon chain tail was varied by carrying out growth in C_{12}TAB. Figure 5 shows that the tail has no significant effect on the critical nucleation size. The chain length does, however, affect the isometric growth rate. Figure 6 clearly demonstrates that the shorter chain C_{12}TAB allows more rapid growth of the seed particles than C_{16}TAB. This is to be expected since the longer tail will create a physically longer barrier through which Au^+ must pass, and an energetically higher barrier due to increased van der Waals binding of the hydrocarbon chain.[20]

Our observations support and enhance the "zipping" mechanism put forth by Murphy and co-workers to explain the affect of the surfactant properties on the nanorod aspect ratio.[20] In that model, the alkyltrimethylammounium headgroup selectively binds different gold facets on the seed particle to create growth anisotropy and the surfactant chains stabilize the bilayers through van der Waals interactions along the nanorod sides. Longer chains lead to more stabilization and therefore longer nanorods. Our data suggest that enhanced growth along the ⟨110⟩ direction begins at a seed diameter of 17 nm and will terminate once the rod diameter reaches 22 nm. Therefore, there is a finite time during which the nanorod can elongate along its ⟨110⟩ fast growth axis. According to Figure 6, the longer chain surfactant slows the isometric growth rate of the particles, so it should also slow the diameter growth rate of the nanorods. This reduced diameter growth rate results in a longer time interval for fast ⟨110⟩ growth, thus producing higher aspect ratio nanorods.

Conclusion

We have described a simple method for the synthesis of gold nanorods on surfaces and applied it to studies of the growth mechanism. We found that the seed particles must grow to a minimum diameter of 17 nm to initiate nanorod formation, and that this minimum was the same for surfactants with 12- and 16-carbon chains. The chain length did, however, affect the isometric growth rate, which was faster for the shorter chain. Altering the surfactant headgroup disrupted the growth anisotropy and produced no nanorods as previously observed in solution-phase experiments. These observations support a recent model explaining the nanorod aspect ratio dependence on the surfactant properties.

Acknowledgment. This work was supported by the Robert A. Welch Foundation and the donors of the Petroleum Research Fund, administered by the American Chemical Society.

References and Notes

(1) Nikoobakht, B.; El-Sayed, M. A. *J. Phys. Chem. A* **2003**, *107*, 3372−3378.
(2) Kovtyukhova, N. I.; et al. *J. Phys. Chem. B* **2001**, *105*, 8762−8769.
(3) Salem, A. K.; Searson, P. C.; Leong, K. W. *Nat. Mater.* **2003**, *2*, 668−671.
(4) Haes, A. J.; et al. *Nano Lett.* **2004**, *4*, 1029−1034.
(5) Haynes, C. L.; Van Duyne, R. P. *J. Phys. Chem. B* **2001**, *105*, 5599−5611.
(6) Hirsch, L. R.; et al. *Proc. Natl. Acad. Sci. U.S.A.* **2003**, *100*, 13549−13554.
(7) Link, S.; El-Sayed, M. A. *J. Phys. Chem. B* **1999**, *103*, 4212−4217.
(8) Foss, C. A.; et al. *J. Phys. Chem.* **1994**, *98*, 2963−2971.
(9) Thurn-Albrecht, T.; et al. *Science* **2000**, *290*, 2126−2129.
(10) Yu, Y.-Y.; et al. *J. Phys. Chem. B* **1997**, *101*, 6661−6664.
(11) Jana, N. R.; Gearheart, L.; Murphy, C. J. *J. Phys. Chem. B* **2001**, *105*, 4065−4067.
(12) Jana, N. R.; Gearheart, L.; Murphy, C. J. *Chem. Commun.* **2001**, 617−618.
(13) Jana, N. R.; Gearheart, L.; Murphy, C. J. *Adv. Mater.* **2001**, *13*, 1389−1393.
(14) Jana, N. R.; Gearheart, L.; Murphy, C. J. *Chem. Mater.* **2001**, *13*, 2313−2322.
(15) Nikoobakht, B.; El-Sayed, M. A. *Langmuir* **2001**, *17*, 6368−6374.
(16) Johnson, C. J.; et al. *J. Mater. Chem.* **2002**, *12*, 1765−1770.
(17) Gai, P. L.; Harmer, M. A. *Nano Lett.* **2002**, *2*, 771−774.
(18) Nikoobakht, B.; El-Sayed, M. A. *Chem. Mater.* **2003**, *15*, 1957−1962.
(19) Sau, T. K.; Murphy, C. J. *Langmuir* **2004**, *20*, 6414−6420.
(20) Gao, J.; Bender, C. M.; Murphy, C. J. *Langmuir* **2003**, *19*, 9065−9070.
(21) Busbee, B. D.; Obare, S. O.; Murphy, C. J. *Adv. Mater.* **2003**, *15*, 414−416.
(22) Taub, N.; Krichevski, O.; Markovich, G. *J. Phys. Chem. B* **2003**, *107*, 11579−11582.
(23) Wei, Z.; Mieszawska, A. J.; Zamborini, F. P. *Langmuir* **2004**, *20*, 4322−4326.
(24) Jin, R.; et al. *Science* **2001**, *294*, 1901−1903.
(25) Bustamante, C.; Keller, D. *Phys. Today* **1995**, *48*, 32−38.
(26) Atkin, R.; et al. *Adv. Colloid Interface Sci.* **2003**, *103*, 219−304.
(27) Yagi, K.; et al. *J. Cryst. Growth* **1975**, *28*, 117−124.